PHILOSOPHICAL TRANSACTIONS OF THE ROYAL SOCIETY A MATHEMATICAL, PHYSICAL & ENGINEERING SCIENCES

Turbulent flux events in a nearly neutral atmospheric boundary layer

Roddam Narasimha, S. Rudra Kumar, A Prabhu and S.V Kailas

Phil. Trans. R. Soc. A 2007 **365**, 841-858
doi: 10.1098/rsta.2006.1949

PHILOSOPHICAL TRANSACTIONS OF THE ROYAL SOCIETY A

Phil. Trans. R. Soc. A (2007) **365**, 841–858
doi:10.1098/rsta.2006.1949
Published online 18 January 2007

Turbulent flux events in a nearly neutral atmospheric boundary layer

By Roddam Narasimha[1,*], S. Rudra Kumar[2], A. Prabhu[3] and S. V. Kailas[4]

[1]*Engineering Mechanics Unit, Jawaharlal Nehru Centre for Advanced Scientific Research, Jakkur PO, Bangalore 560 064, India*
[2]*VectorMax India Pvt. Ltd, Indira Nagar, Bangalore 560 038, India*
[3]*Indian Institute of Science, Bangalore 560 012, India*
[4]*Abstract Algorithm Technologies Pvt. Ltd, Hebbal, Bangalore 560 024, India*

We propose here a novel method of analysing turbulent momentum flux signals. The data for the analysis come from a nearly neutral atmospheric boundary layer and are taken at a height of 4 m above ground corresponding to 1.1×10^5 wall units, within the log layer for the mean velocity. The method of analysis involves examining the instantaneous flux profiles that exceed a given threshold, for which an optimum value is found to be 1 s.d. of the flux signal. It is found feasible to identify normalized flux variation signatures separately for positive and negative 'flux events'—the sign being determined by that of the flux itself. Using these signatures, the flux signal is transformed to one of events characterized by the time of occurrence, duration and intensity. It is also found that both the average duration and the average time-interval between successive events are of order 1 s, about four orders of magnitude higher than a wall unit in time. This episodic description of the turbulence flux in the time domain enables us to identify separately productive, counter-productive and idle periods (accounting, respectively, for 36, 15 and 49% of the time), taking as criterion the generation of the momentum flux. A 'burstiness' index of 0.72 is found for the data. Comparison with laboratory data indicates higher (/lower) ejection (/sweep) quadrant occupancy but lower (/higher) contributions to flux from the ejection (/sweep) quadrant at the high Reynolds numbers of the atmospheric boundary layer. Possible connections with the concept of active and passive motion in a turbulent boundary layer are briefly discussed.

Keywords: turbulent momentum flux; flux events; atmospheric boundary layer; burstiness; episodic description

1. Introduction

Since the identification of the quasi-cyclic character of turbulent energy production, called the bursting phenomenon in the turbulent boundary layer by Kline *et al.* (1967), there has been a considerable effort at providing a physical

* Author for correspondence (roddam@caos.iisc.ernet.in).

One contribution of 14 to a Theme Issue 'Scaling and structure in high Reynolds number wall-bounded flows'.

description of the structure of the flow in terms of 'coherent' motions involving various elements such as low-speed streaks, quasi-streamwise vortices, etc. This effort has involved both extensive experimental investigations, using PIV (particle image velocimetry) in recent years (e.g. Guala *et al.* 2006), and direct numerical solutions of the Navier–Stokes equations (e.g. Hoyas & Jimenez 2006). The present work proceeds along the line of quantitative studies that depend essentially on the use of signal-processing techniques as a tool for inferring scaling laws and hence helping to unravel the nature of the mechanism behind the quasi-cyclic production of flux. One class of these studies is concerned with the identification of events from time-series data of velocity components or other variables, going back to early work using a variety of techniques such as band-pass filters (Rao *et al.* 1971), VITA (varying interval time average; Blackwelder & Kaplan 1976), wavelets (e.g. Farge 1992), etc. Much debate has taken place on the frequency of such events and their scaling (Rao *et al.* 1971; Blackwelder & Haritonidis 1983; Narasimha & Kailas 1987; Antonia & Krogstad 1993; Kailas & Narasimha 1994; to quote only a few relevant references). A second class of studies has examined turbulent fluxes and has proceeded from the early and pioneering work of Willmarth & Lu (1972) and Lu & Willmarth (1973) emphasizing quadrantal analysis in the plane of the streamwise and wall-normal velocity components, based on threshold settings and conditional sampling.

Following the initial studies in laboratory flows, there have been some interesting investigations of coherent motion in the atmosphere, where extremely high Reynolds numbers, Re (of order 10^7–10^8 based on boundary layer thickness), are achievable. Phong-anant *et al.* (1980) used simultaneous temperature traces at several heights to detect organized structures in the atmospheric surface layer and obtained signatures of velocity and temperature fluctuations and their products that were 'qualitatively similar to those in the laboratory boundary layer'. Schols (1984) used the VITA technique on temperature traces to obtain conditionally sampled signatures of various atmospheric parameters; contributions from these signatures to the mean momentum transport were reported to be around 30–50%. Liandrat & Moret-Bailly (1990) used wavelets for a study of active periods in atmospheric turbulence. Narasimha & Kailas (1987) presented an early review, along with new results on energy events in the atmospheric boundary layer. As they pointed out, to anybody who examined high Re atmospheric data even two decades ago, arguments about near-wall phenomena scaling exclusively on wall variables acting as agents driving boundary layer flow would have appeared unsupportable by experimental evidence.

A logical question that arises from all this work, and the one that we propose to address here, is how far one can take a description of turbulent flux time-series in terms of 'events' of one kind or another (Narasimha 1990). More specifically, given the time-series of a fluctuating turbulent quantity at a point $\boldsymbol{x}$ as a function of time t, one can ask whether, instead of the classical description of the field in terms of generalized harmonic analysis, an alternative description that may be termed 'episodic' is feasible. Such an episodic description would seek suitable definitions of event types, magnitudes, arrival times, etc. and may be thought of as providing an extended 'point-process' description of the flux signal. (In the simplest case, a point process is realized by a series of point events; but we shall need to attach a set of variables to each event, as will be seen in §5.) Whether

such a description renders the problem more tractable in terms of solving the Navier–Stokes equations is not clear, but it is certain that there are many situations where an episodic description would be more useful. For example, an understanding of turbulent events may have advantages in the use of active control techniques; in geophysical situations, insight into events is important in the problem of assessing the frequency of large deviations, especially in view of the prevalence of non-Gaussian tails (e.g. Narasimha 1990) which has significant implications; the prediction of 'big' events raises fundamental questions (Ramage 1980).

Some preliminary attempts in this direction have already been made. In particular, Narasimha & Kailas (1990) introduced two concepts in such an episodic description. The first involves the extraction from the original time-series of a 'chronicle' of events, which occur at instants marked along the time axis; from a preliminary analysis using the VITA technique on the velocity components, they identified more than one type of event. The second concept introduces a parameter called 'burstiness', which is a measure of how compact in time and significant in contribution the events so detected are, in relation to a flow quantity of interest such as energy or flux. This involved a hierarchy of events ordered by magnitude (defined in some appropriate way), and an analysis of the duration of each event so ordered. The burstiness (to be discussed further in §5*e*) could vary, in this definition, from zero when the contributions are distributed evenly over time to unity when they occur entirely in instantaneous events (of vanishing duration). For the energy of streamwise velocity fluctuations, the burstiness in a near-neutral atmospheric surface layer was reported by them to have a lower bound in the neighbourhood of 0.3–0.4.

Now, although the fluxes are crucial to an understanding of turbulent shear flow, flux time-series have not attracted the attention they deserve. In attempting such an analysis, we must remember two issues that are peculiar to the fluxes. First, unlike energy or dissipation, a turbulent flux (whether of momentum, energy, concentration or any other quantity of interest) is not sign definite: at any given instant, it can in general be either positive or negative. Even the sign of the mean flux, which is related to that of the gradient of the associated variable in most turbulence models, cannot be considered known always, as counter-gradient fluxes do occur in many flows. Second, whatever elements may be used to describe the flux time-series, the greatest interest attaches to evaluating the contributions of the elements to the *mean* flux (positive or negative), rather than to the mean square of the fluctuations around the mean. Most tools in common use for stochastic analysis are not suited to handling questions of this type. This applies to generalized harmonic analysis as well as to wavelets. In particular, the admissibility condition for a wavelet function requires that its mean must be zero, which precludes it from describing its contribution to the *mean* flux.

We attempt here an episodic description of turbulent flux processes in an atmospheric boundary layer. This is particularly interesting owing to the relative ease with which fluxes can be directly measured and owing to the high Reynolds numbers achievable in such flows. The quest for an episodic description involves several steps: an event detection procedure; a classification of event types; a determination of a sufficient number of parameters to characterize the event; a representation of the original process as a suitable chronicle; and, finally, the

investigation of the appropriate statistics under various flow conditions. We consider each of these steps in turn in the rest of the paper. The motivation for such an analysis is the expectation that the scaling of event parameters would shed light on possible mechanisms of stress generation. This approach incidentally suggests a way of making a *temporal* analysis of the velocity in terms that may be related to notions of active and passive motion.

2. Data analysed

Data used for the present investigation are taken chiefly from the Monsoon Trough Boundary Layer Experiment (MONTBLEX), carried out in India during the summer of 1990 (Goel & Srivastav 1990; Narasimha *et al.* 1997). Some supplementary data from the 300 m tower of the Boulder Atmospheric Observatory (BAO), Colorado, USA (Kaimal & Gaynor 1983; Narasimha *et al.* 1990) and the 200 m tower of KNMI at Cabauw, The Netherlands (Driedonks *et al.* 1978) will also be used.

The MONTBLEX project included masts at four different sites for surface layer observations. Data were recorded at 8.41 Hz, in stretches of 10–15 min every hour during intensive observation periods (passage of low-pressure systems, etc.), and for the same duration every 3 h at other times. A detailed report on the set-up, observations and the quality of the data is available in Rudra Kumar *et al.* (1997). A variety of checks, including many suggested by Kaimal (1990), show the quality of tower data to be high. As an example, there was excellent agreement between sonic and cup anemometers in data on the horizontal wind speed. As observations at Jodhpur provided the most extensive sets of good continuous data, many of the results described in this paper use data from this site. In particular, the flux data used in the present investigation are derived from the three wind velocity components and temperature measured by a sonic anemometer (Applied Technologies, Inc., USA) placed at a height of 4 m above ground, which corresponds to 1.1×10^5 wall units and something like a hundredth of the boundary layer thickness.

In the present paper, attention is largely confined to near-neutral conditions, with a bulk Richardson number of -0.05 over the mast and a flux Richardson number of -0.06 at $z=4$ m. From an analysis of the flow at other stability conditions (Rudra Kumar *et al.* 1993) as well as the results of other work on atmospheric boundary layers (e.g. Stull 1990), the flow conditions selected for analysis are effectively close to neutral. Table 1 lists relevant information about the site at Jodhpur and the conditions under which the data chiefly analysed here were recorded. The data from the BAO and the Cabauw Meteorological Observatory towers have been acquired when the stability conditions were extremely close to neutral. Use of data from different locations under near-neutral conditions enables comparison of results for variation (if any) due to site-specific conditions. Results for non-neutral conditions will be reported separately.

3. Some preliminary observations

To begin with, we present in figure 1 a series of streamwise velocity time traces from cup anemometers at the six levels of the Jodhpur mast, chiefly to compare them qualitatively with other such traces at relatively lower Reynolds numbers, in

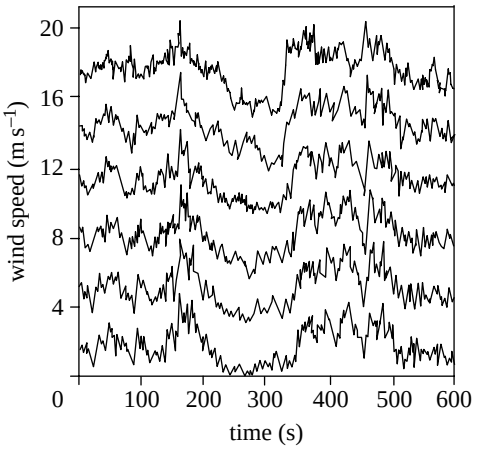

Figure 1. Wind speed records from cup anemometers mounted on the Jodhpur mast at 1, 2, 4, 8, 15 and 30 m above ground (file J6261400).

Table 1. Basic data on test site and flow conditions.

site	Jodhpur, India (26° N, 73° E) Campus of Central Arid Zone Research Institute
surface	short grass and moss[a] flat, open in prevailing wind direction (200–230°)
average roughness length	12.3 mm in 'smooth' sector covering prevailing wind
time of observation	30 June 1990
prevailing weather	dry, overcast sky, just before monsoon onset
height of instrumentation	z=4 m, $z_+ = 1.1\times10^5$, $z/\delta = O(10^{-2})$
mean wind speed	3.15 m s^{-1}
friction velocity U_*	0.437 m s^{-1}
wall units (U_*, ν)	0.083 ms, 0.036 mm
overlap layer units (U_*, z)	9.2 s, 4 m
outer units(U, δ)	∼30 s, ∼400 m
bulk Richardson number, 0–30 m	−0.05
flux Richardson number at 4 m	−0.06
Obukhov length	−182 m

[a]The method of characterization follows the work of Wieringa (1993).

particular Antonia *et al.* (1990, fig. 6). The latter data, taken in a wind tunnel at a boundary layer thickness Reynolds number $Re_\delta \simeq 19\times10^3$, present eight traces beginning from $z_+ = 17.3$, $z/\delta = 0.025$ and ending at $z_+ = 415$, $z/\delta = 0.60$, where z is the height above surface, δ is the boundary layer thickness and subscript + indicates wall units. The present atmospheric data correspond to $Re_\delta \simeq 10^7$, $z_+ = 27.5\times10^3$ to 0.825×10^6, $z/\delta = O(10^{-2})$. (In the absence of direct observations, a rough estimate of boundary layer thickness has been made based on radio-sonde and sodar data (Rajkumar *et al.* 1997) and of a reference velocity (12 m s^{-1}) based on the former.) These traces show that there can be hardly any question about the existence of strongly coherent motions even at very high Reynolds numbers. Furthermore, the characteristic time-scales are of order 10^1–10^2 s (approx. 10^5–10^6 wall units, $O(1)$ overlap layer or outer unit),

and length-scales of at least 30 m (approx. 10^6 wall units, 10^{-1} outer unit; see table 1). It is thus even qualitatively clear that at very high Reynolds numbers, there are strong coherent motions of large temporal and spatial scales in the log layer even at heights that are a small fraction of the boundary layer thickness. At the same time, the top-most trace in the figure is taken at a height $z=30$ m, which is approximately $z_+ = 8.25\times10^5$ wall units. At the time of these measurements, the velocity closely followed the standard log law (Rudra Kumar *et al.* 1997), so the data may be taken to represent flow in the lower part of the inertial sub layer.

The momentum flux data used here are obtained from a sonic anemometer that provides all the three components of the wind speed at 4 m above ground. The instantaneous momentum flux is the product $-u'w'$, where u' is the resultant velocity fluctuation in the streamwise direction, computed from the two horizontal components measured by the sonic anemometer, and w' is the normal velocity. As may be judged from figure 1, u' often tends to remain of one sign for periods of order 10–20 s, whereas w' (not shown) experiences many more zeros. The instantaneous flux signal reveals short periods of intense activity during which the signal is frequently an order of magnitude larger than the mean. (Willmarth & Lu 1972 report an event which at its peak had a flux 62 times the mean.) We shall call these periods of activity 'flux events'. Detection and characterization of these events is one major objective of this paper.

An event will be called positive (/negative) if its contribution to the flux $-\overline{u'w'}$ is positive (/negative). The second and the fourth quadrants will contain positive events and the other two negative events.

4. Detection techniques

(a) *Different detectors*

Different signal-processing techniques have been considered here in order to detect bursts or events in the time-series being analysed. The first is an improvement of the VITA technique that removes the arbitrariness in the choice of averaging time, t_{av}, and threshold, k. The improvement (Kailas & Narasimha 1994) is based on the discovery of a certain kind of similarity in which the frequency of detected events is independent of t_{av} *over* a range of values of k in atmospheric (high Re) data.

A second method involves a crucial modification of the simple one-parameter threshold technique of Lu & Willmarth (1973). The Lu & Willmarth threshold is defined by a hyperbolic 'hole' whose size in the $u'w'$ plane is a multiple of the mean flux. However, as we have already seen, the fluctuations in the $u'w'$ product can be a huge multiple of the mean (it can even tend to infinity as a flow approaches separation). We have found that the r.m.s. value is a far more appropriate threshold, in particular owing to the insensitivity of the results to a threshold less than 1 s.d. (figures 4 and 9). In this scheme of detection, an event is said to occur when

$$|f| > k_f \hat{f}, \tag{4.1}$$

where f is $-u'\ w'$ for momentum flux; $\hat{f}$ is its r.m.s. fluctuation; and k_f is a positive multiplier setting the threshold. When equation (4.1) holds for an unbroken sequence of temporal samples, we count only one event for the set of samples.

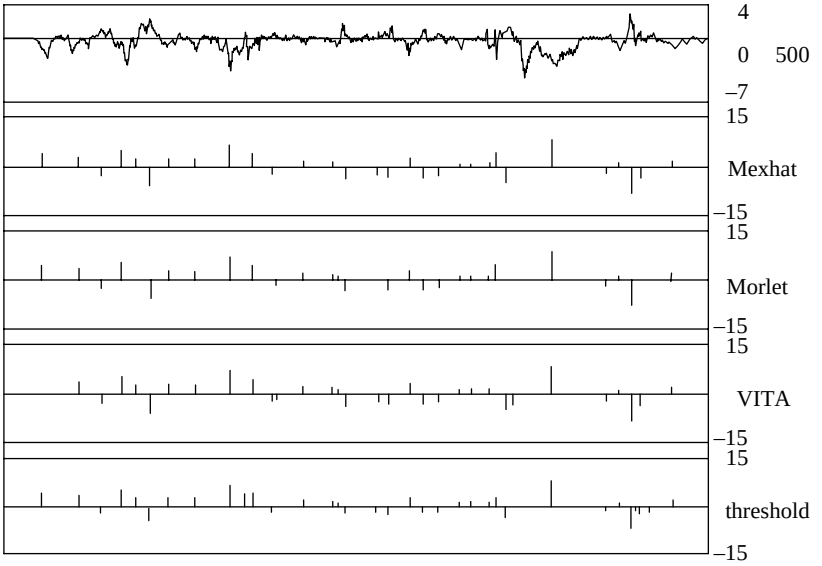

Figure 2. Event markers from different methods of event detection.

The Lu & Willmarth threshold does *not* lead to a compact description of the kind we offer here.

A third method that is due to Kailas & Narasimha (1996, unpublished; see, however, Anandakumar & Kailas 1999) uses a threshold on the wavelet transform as an event detector. In this method, the continuous wavelet transform coefficients for the whole data stretch are determined at the dyadic time-scales 2^n s, $n=1, 2, 3 \ldots$ (A special program called NALLETS, written by S. V. Kailas, was used for this purpose.) The local maxima of the absolute magnitude of the coefficients are then determined at each wavelet scale. A local maximum is considered a detected event if the peak flux at the time of occurrence of the maximum exceeds the r.m.s. value of the flux. This results in a unique set of events like the ones shown in figure 2, where results for both Mexican hat and the Morlet wavelet are shown. It is seen that there is good agreement between the results from either wavelet. (Note that the detection algorithm used here is different from that of Kaspersen & Krogstad (2001), who start from squared wavelet coefficients. However, they use the u-velocity signal alone, select a dominant scale around the peak in the co-spectrum, but use no discrimination on the peak level or event duration. The present scheme, on the other hand, starts with the $u'w'$ signal, no *a priori* choice of scale is made, but a threshold is set on the magnitude of the peak flux, which should exceed the r.m.s. value $\hat{f}$ of the flux to detect an event, following the same reasoning as above.)

Figure 2 shows event markers for a stretch of data on the momentum flux signal $-u'\ w'$ from the techniques described above. The instants of time locating the events constitute a simple point process (Cox & Isham 1980), but we attach to the marker a height proportional to the intensity of the event, defined in a way that will be described below in greater detail.

What is remarkable in figure 2 is that all the detector functions used agree so closely among themselves. There are some differences, however: the Mexican hat

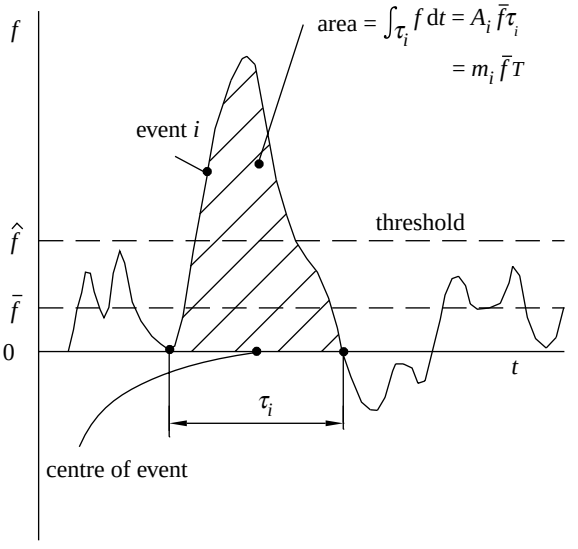

Figure 3. Sketch defining event parameters.

wavelet detects 30 events, Morlet only 27, VITA 31 and flux threshold 35, all of the same order, but clearly the threshold method captures events that are missed out by the others.

However, although all techniques are comparable on providing event markers, there are difficulties in assigning *intensities* to the detected events in the VITA and wavelet techniques, as they cannot quantify contributions to the *mean* flux. On the other hand, the simple flux-threshold technique, with certain further refinements that we shall describe below, proves extremely effective. We have therefore adopted this technique in the analysis that follows.

(*b*) *Development of the threshold technique*

To characterize the flux events detected by the threshold technique, we first define the duration τ_i of each event i as the time-interval between the zeros in $u'w'$ closest to the sequence of samples satisfying condition (4.1), and the centre of the event as the mid-point of the duration (figure 3). This procedure results in a well-defined flux event, as may be seen from the average flux profiles presented in figure 5. We define two more parameters that are used throughout this investigation. Firstly, the (non-dimensional) amplitude A_i of a flux event i is defined as

$$A_i = \frac{1}{\bar{f}} \int_{\tau_i} f \frac{\mathrm{d}t}{\tau_i}, \tag{4.2}$$

where the integral is evaluated over the duration τ_i of the event around its centre and $\bar{f}$ is the mean value of the flux. The amplitude is thus the ratio of the average flux generated over an event to the long-term mean flux. Secondly, the (fractional) contribution from an event i to the total flux, defined as its magnitude, is

$$m_i = \frac{A_i \tau_i}{T}, \tag{4.3}$$

where T is the total duration of the data stretch. Thus, of two events which have the same amplitude, the longer one has a greater magnitude.

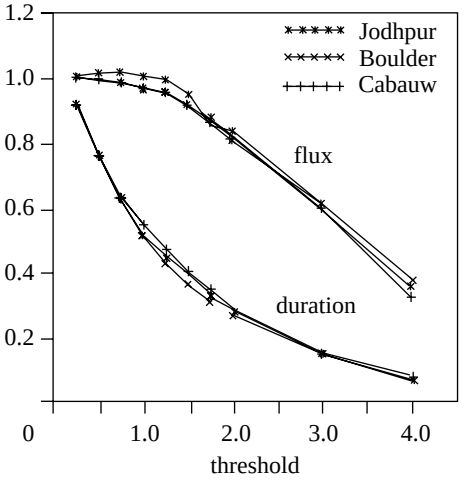

Figure 4. Variation of fractional contribution to flux and fractional cumulative duration of corresponding flux events as function of threshold for event detection in multiples of r.m.s. value of flux fluctuation. Measurement at height above ground of 4 m at Jodhpur, 10 m at Boulder and 20 m at Cabauw.

As may be seen from the above definitions, the existence of a well-defined optimal value for the threshold k_f is crucial in this method. In figure 4, we plot the cumulative contribution from the events to the total flux for various values of the threshold, with data from three different sources: Jodhpur; Boulder; and Cabauw. It is obvious that if $k_f=0$, the events detected would have to account for all the flux generated, but what is remarkable about the data of figure 4 is that there is a range of k_f (up to about unity in this case) over which the total contribution roughly remains constant and stays close to 100%, i.e. up to a certain value of k_f, the events detected as exceeding that threshold account for virtually all the flux. The different datasets are in good agreement with each other and show that the criterion we identify is robust. We obtain a minimal description by choosing a value of k_f that will lead to the identification of the smallest number of events that account for all the flux. (The additional events identified by the adoption of a threshold $k_f<1$ will clearly be relatively small and cancel each other out; they can be thought of as 'noise' in the flux process.) As events below a threshold of unity account for virtually all of the flux, the value $k_f=1$ provides the optimum we are seeking. In general, this threshold is found to be in the range of 1–1.5 depending on the stability conditions in the atmosphere.

Figure 4 also shows the fraction of the duration occupied by the events for the same three datasets. Consistently with the above argument, the cumulative duration drops steeply with increase in threshold, and it is seen that events occurring over only half the time or less account for all the flux.

5. Momentum flux events under nearly neutral conditions

We first discuss in detail various characteristics of momentum flux events detected in a typical dataset recorded under near-neutral conditions. The file, J6301200, has been selected here for this purpose (the code identifies the data as recorded at Jodhpur at 12.00 h local time on 30 June 1990). The duration of the

Table 2. Quadrant statistics for momentum flux events (%).

parameter	present work	Antonia (1977)	Schwarz-van Manen (1993)	Willmath & Lu (1972)
quadrant occupancy				
Q1	16	17	19	17
Q2	34	32	30	29
Q3	22	16	19	18
Q4	28	35	32	36
flux contribution				
Q1	−29	−16	—	−10
Q2	+68	+67	—	+80
Q3	−18	−18	—	−14
Q4	+79	+67	—	+44

data stretch is 10 min. The winds during this time were from south–southwest with an average magnitude of 3.2 m s^{-1}, the mean direction being 195° from the north. The gradient Richardson number for the 1–30 m slab is −0.05 and the flux Richardson number computed at 4 m is −0.06. The ratio of the height at which the measurements were made (z=4 m, $z_+ = 1.1 \times 10^5$) to the Obukhov length L is $(z/L) = -0.02$. These stability parameters indicate near-neutral conditions (Stull 1990; Kaimal 1990). In addition, from the synoptic conditions recorded along with the data file, it is known that during the time of data acquisition the sky was overcast, which aids in creating a nearly neutral surface layer during daytime (see Rajkumar *et al.* (1997) for a detailed discussion of the stability characteristics of the boundary layer at the site).

(*a*) *Quadrant statistics*

Quadrantal analysis in the $u'w'$ plane gives us two simple statistics: the fraction of $u'w'$ data samples—or quadrant 'occupancy' as we shall call it—and the contribution to the flux from each quadrant.

Comparison with similar statistics from earlier investigations (e.g. Willmarth & Lu 1972; Antonia 1977; Schwarz-van Manen 1993) is presented in table 2. Schwarz-van Manen's data come from the 200 m Cabauw tower (mentioned in §1). The duration of the data stretch is 13 min, taken when the stability conditions were near-neutral. Antonia's data were taken at a small height (1.48 m) above a wheat crop canopy near Bungendore (New South Wales), recorded when the stability was near-neutral or slightly unstable. The laboratory data of Willmarth & Lu come from experiments conducted in the 5 in. thick boundary layer that develops on the smooth floor of the 5×7 ft low-speed wind tunnel of the Department of Aerospace Engineering at the University of Michigan, at a height of 30 wall units and at a Reynolds number of 4.7×10^4 based on the boundary layer thickness.

One may discern some weak trends in the quadrant occupancy: all the high Re atmospheric data show slightly higher Q2 ejection occupancy and slightly lower Q4 sweep occupancy. There are bigger changes in the flux contributions: appreciably less from Q2 ejections, and substantially more from Q4 sweeps and

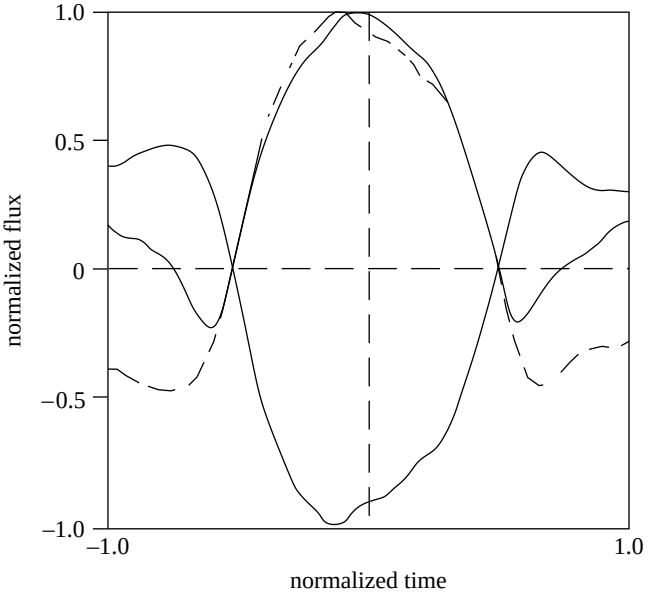

Figure 5. Normalized signatures of positive (upper) and negative (lower) events with threshold technique. Dotted line is a mirror reflection of the negative event about the horizontal axis.

the Q1, Q2 counter-productive quadrants. The trends are the same in both the present data and from Antonia, although there is a significant difference between the two in Q1 flux.

The contribution to the total flux from Q2 and Q4 varies over the range 124–147%, the lowest value coming from the lower Reynolds number flow. Given the different site conditions, the atmospheric data are in reasonable agreement among themselves, and there is a strong suggestion that at higher Re, sweeps contribute more and ejections less to the total flux.

(*b*) *Event signatures*

A simple conditional averaging over all the detected events produces no strong signature, indicating partial cancellation between positive and negative events. When they are separately considered, on the other hand, a well-defined mean signature is seen for each type of event, with a peak at the centre.

However, it is most appropriate to do the averaging of events taking into consideration their respective intensities and durations, which vary from event to event. Thus, an alternative way of averaging which results in defining more clearly the mean structure of the events is as follows. The time axis is normalized for each event by its own duration, and the amplitude by the respective peak value during the event. A normalized signature is then obtained by averaging the normalized amplitude variable at each value of the normalized time. These averages are shown for both positive and negative events in figure 5. It is found that, as the threshold is varied, event profiles converge to a unique signature in what may be called the core of the event, i.e. the portion of it that lies between the zeros. The wings however are less insensitive to the threshold, especially in

Table 3. Momentum flux-event statistics.

data set	J6 301200
mean momentum flux	0.191 $m^2\,s^{-2}$
ratio r.m.s./mean	3.04
event frequency	0.73 s^{-1} in Q1
	0.28 s^{-1} in Q3
	0.92 s^{-1} in Q2
	1.42 s^{-1} in Q4
productive period	36%
counter-productive period	15%
idle/passive period	49%
average duration of:	
positive events	1.71 s
negative events	1.12 s
average peak flux in	
positive events	0.50 $m^2\,s^{-2}$
negative events	-0.34 $m^2\,s^{-2}$
wall unit, time	0.083 ms
outer unit, time	$\sim O(30\,s)$

negative events, but always have a sign opposite that of the core. Part of the reason for the variability in the wings is the interference from neighbouring events. Interestingly, both the types of event have a structure that looks qualitatively similar except for a change in sign, but there are some quantitative differences in the wings of the event profile, as can be seen from the negative event signature plotted as a dotted line with sign reversed in the figure. The wings of the positive event have both positive and negative parts, so the total contribution to flux largely comes from the central core of the event. The negative event does not have this characteristic, and a proper treatment of its wings poses certain difficulties which need further investigation. Overall, however, both the event types have a signature akin to a Mexican hat profile with a non-vanishing mean.

(*c*) *Event parameters*

We now present results for momentum flux events detected using the threshold technique discussed in §3. There are three parameters that characterize each event, viz., amplitude, magnitude and duration; a fourth important parameter of the event *process* is their inter-arrival times. These and other related parameters are listed in table 3. It is seen that both the average inter-arrival time between events and their duration are of order 1 s, to be compared with a wall time unit of order 10^{-4} s, an overlap unit of order 10 s and an outer time unit of order 30 s. It has already been pointed out that no direct measurement of boundary layer thickness was made at the site. Comparison with radio-sonde data on wind speed (Rajkumar *et al.* 1997) and sodar and other measurements on the structure of the boundary layer under conditions similar to those prevailing in the selected test period suggest edge velocity $U \simeq 10$–12 m s^{-1} and boundary layer height any where between 200 and 600 m, with 400 m as the best guess. Hence, the outer time-scale is only a very rough

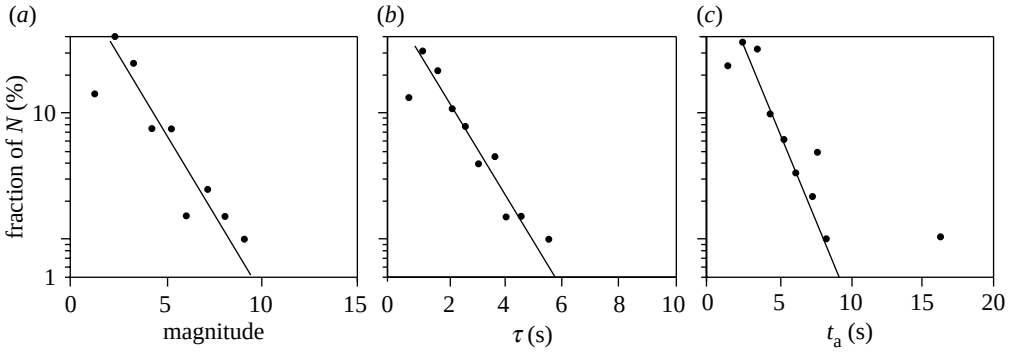

Figure 6. Frequency distribution of (*a*) event magnitude, (*b*) event duration and (*c*) inter-arrival times (N=number of events detected).

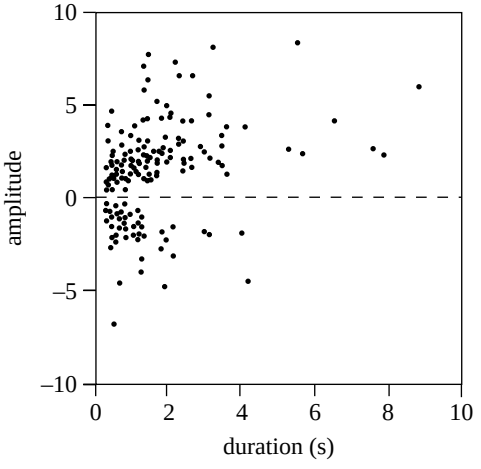

Figure 7. Cross-plot of event amplitude (arb. units) and event duration.

estimate and can vary over a wide range from as low as 10–15 s to nearly 50 s. Nevertheless, the vast disparity between event time-scales and the wall unit can be said to rule out decisively an exclusive dependence of flux generation events on wall flow. The discrepancy between event time-scales and outer flow scales is therefore much less severe, but some weak mixed scaling law cannot be ruled out.

Figure 6 shows the probability distributions of the above flux parameters. Although the data stretch (10 min) is not long enough to eliminate some scatter, the nature of the distributions is quite clear. All of them suggest that an exponential distribution may not be a bad approximation at low parameter values, i.e. for short, relatively weak events. An exponential distribution for the inter-arrival times is consistent with the part of the chronicle corresponding to short inter-arrival times being an example of a Poisson process (Cox & Isham 1980).

Figure 7 shows plots of the amplitude versus duration for all the events in the same data stretch. It is clear that there is a wide range of values of the amplitude for any given event duration, and vice versa. The magnitude of the events shows a similar behaviour. Thus, the *size* of the event and its duration are best considered to be two distinct parameters.

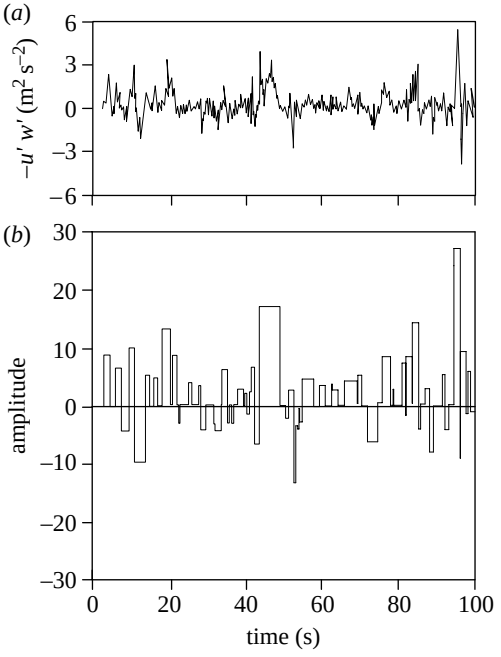

Figure 8. (*a*) Instantaneous flux signal time-series and (*b*) its representation as a chronicle of events.

(*d*) *Flux-event chronicle*

We may now obtain a chronicle of flux events representing the flux time-series in terms of the parameters defined above. Figure 8 shows such a chronicle for a momentum flux time-series of 100 s duration (using $k_f = 1$) from Jodhpur. It will be seen that the chronicle contains both positive and negative events, each event being represented by a rectangular pulse whose width indicates duration τ_i, height indicates the amplitude A_i and area indicates total flux contribution m_i. The threshold technique used here accounts for all the flux generated, as we shall shortly reconfirm.

(*e*) *Burstiness*

Using an improvement of a procedure first proposed by Narasimha & Kailas (1990), we shall now determine quantitatively a parameter that may be called the burstiness in the flow. This parameter provides a measure of how compact and significant the events detected in the time-series are, in terms of their contribution to a flow quantity of interest, such as, for example, the energy or mean square value in the case of time-series for single variables like u', w', T', etc. or the mean flux in the case of products like $u'w'$. The procedure is as follows. First, the contribution from each event, i, to the flow quantity of interest, say q, is determined from equation (4.3). Then, all the events are ordered downwards in magnitude from the biggest contributor. The cumulative contribution to the quantity, q, from this ordered sequence of events is plotted against their cumulative duration, normalized, respectively, by the mean value of q and the total duration of the data stretch.

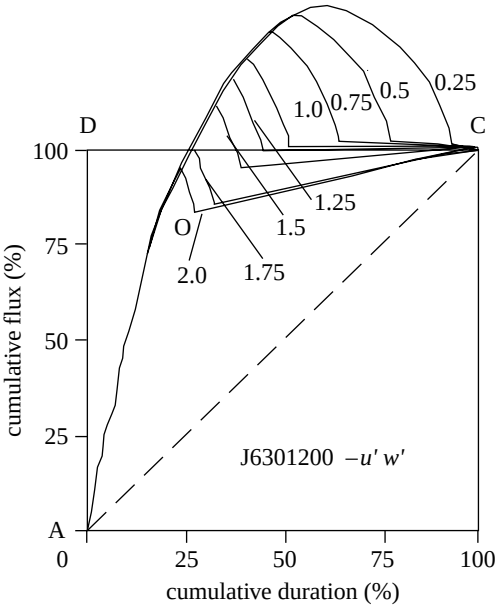

Figure 9. Variation of cumulative flux with cumulative event duration at different values of threshold for event detection in units of r.m.s. value of flux fluctuation.

The resulting burstiness curve, as we shall call it, will take a path of the kind shown in figures 9 and 10. The dashed diagonal line AC in figure 9 represents the line of even contribution in time to the flux (equal time-intervals during the stretch making on average the same contribution to the total flux). If the events were all instantaneous (i.e. their individual and hence also total duration is zero, so the chronicle would be a sequence of delta functions), the burstiness line would have coincided with the vertical axis AD. The events detected may not always account for all of q, in which case the burstiness curve usually ends at a point below the 100% flux line.

There are now two possibilities. If q is positive definite, say for example, the energy, the curve AO may lie within the triangle ADC, as in the case of energy (Narasimha & Kailas 1990): the events detected may not account for all the energy. If q is not sign definite (like the fluxes, for example), we may now proceed in one of two ways. In the first, the ordered sequence of events proceeds from the biggest positive event through to negative events (by signed magnitude). This produces a burstiness curve that reaches a maximum above unity and is brought down thereafter by the contribution of negative events, as in figure 9, which shows curves for different values of the threshold k_f, or in figure 10*a* ($k_f = 1$). The magnitude of the dip due to the negative events indicates their relative contribution with respect to the positive events at each value of k_f. The second way is to order the events by absolute magnitude, without regard to their sign. In this case, the burstiness curve will often have some sharp discontinuities, as illustrated in figure 10*b*. The burstiness factor is defined as the ratio of the area between the curve and AC to the area of the triangle ADC.

Let us return to figure 9 that shows the burstiness curves obtained for the momentum flux as the threshold factor k_f is varied from 0.25 to 2.0. For $k_f \geq 1.25$, the events detected do not account for all the flux, and so constitute an

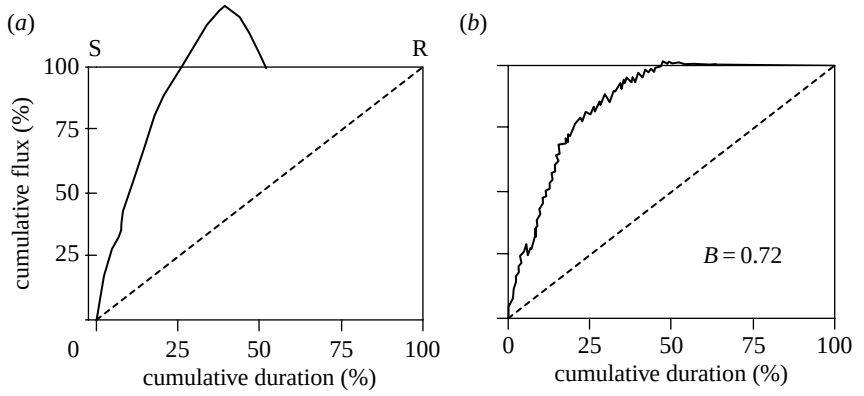

Figure 10. Burstiness curves, with flux events defined with a threshold at 1 s.d. of the flux fluctuation. Events ordered according to (*a*) signed magnitude, from the highest positive through zero to the lowest negative, and (*b*) absolute value of magnitude.

incomplete set in the sense that (the missed) weaker events still contribute significantly to the total flux. On the other hand, with events which have $k_f \leq 1.0$, the flux is all accounted for, but the weak events near the peak of the burstiness curve make no net *additional* contribution to the flux; we may say that there is a 'detailed balance' between weak positive and negative events in this region, the two cancelling each other out. Figure 9 reconfirms the optimality of the choice $k_f \simeq 1$, leading to the smallest number of events that account for all the flux.

In the case shown in figure 10*a* ($k_f = 1$), which is typical for nearly neutral boundary layers, the contribution to the flux from positive events reaches about 125% occupying about 38% of the time and the negative events contribute about −25% to the flux in about 18% of time. We shall call these (active) event periods 'productive' and 'counter-productive'; it is interesting to note that for about 44% of the time, what activity there is consists of weak events of opposite signs that generate zero net flux. They represent a kind of noise and constitute an effectively 'idle' or passive period as far as flux generation is concerned.

In figure 10*b*, the burstiness curve is constructed using the absolute magnitude of each flux event (i.e. ignoring its sign; this accounts for the dips in the curve, which occur when we encounter a negative event in the sequence ordered according to absolute magnitude). The burstiness factor is found to be $B = 0.72$. This value is much larger compared with the typical value of around 0.3 obtained by Narasimha & Kailas (1990) for the energy, using the VITA method (with $t_{\mathrm{av}} = 10$ s and $k = 1$). The reasons for this result are partly in the difference in the procedure used for recognizing the events and the computation of the event duration, and partly in the fact that stress generation is in fact a far burstier phenomenon.

6. Concluding remarks

We have presented here an objective way of distinguishing between productive and counter-productive events and periods (from the point of view of flux) in the time domain, and of identifying idle periods (the blank intervals on the time axis in figure 8). There is the question of the relation of this idea to the concept of active and inactive motions introduced by Townsend. The very simple criterion

we have found is that low-flux fluctuations (typically less than a standard deviation in the flux) make little net contribution to the mean flux, and so could perhaps be identified with passive motion; the more intense fluctuations are 'active' in a generation of flux. An attractive possibility is that the passive motion is best described in the language of waves, whereas the active motions—productive or counter-productive—are best seen as a series of events, possibly related to certain coherent motions. On the basis of the present analysis, no specific connection with any of the coherent structures can be established. But it is clear that the time-scales associated with them are bigger than the wall unit by several orders of magnitude. Furthermore, considering that the time-scales in the fluxes during idle periods are shorter than in the productive motions, there is the possibility that their time-scales are closer to the wall units, at least at large values of z_+ and small values of z/δ, but this proposal requires further study.

We are grateful to Dr J. C. Kaimal for furnishing near-neutral atmospheric boundary layer data from the Boulder Atmospheric Observatory and to Prof. Franz Nieuwstadt and Dr Addie Schwarz-van Manen for similar data from the Cabauw Meteorological Observatory tower. The experiments at Jodhpur were supported by the Department of Science and Technology as part of MONTBLEX 90, and further analysis by the Defence Research and Development Organization through project RN/4124. The assistance of Mr Syed Ameenulla in designing, building and operating the instrumentation during the Jodhpur field experiment is gratefully acknowledged. Figures 1, 7, 8 and 10 appeared in a brief summary of a lecture by R.N. (Narasimha 1995) and are reproduced by permission of the Current Science Association.

References

Anandakumar, K. & Kailas, S. V. 1999 Statistical discrete gust analysis of tower-based atmospheric turbulence data for aircraft response studies. *J. Aerosp. Eng.* **213**, 143–162.

Antonia, R. A. 1977 Similarity of atmospheric Reynolds shear stress and heat flux fluctuations over a rough surface. *Bound. Layer Meteorol.* **12**, 351–364. (doi:10.1007/BF00121471)

Antonia, R. A. & Krogstad, P. A. 1993 Scaling of the bursting period in turbulent rough wall boundary-layers. *Exp. Fluids* **15**, 82–84.

Antonia, R. A., Bisset, D. K. & Browne, L. W. B. 1990 Effect of Reynolds number on the topology of the organized motion in a turbulent boundary layer. *J. Fluid Mech.* **213**, 267–286. (doi:10.1017/S0022112090002324)

Blackwelder, R. F. & Haritonidis, J. H. 1983 Scaling of the bursting frequency in turbulent boundary layers. *J. Fluid Mech.* **132**, 87–104. (doi:10.1017/S0022112083001494)

Blackwelder, R. F. & Kaplan, R. E. 1976 On the wall structure of the turbulent boundary layer. *J. Fluid Mech.* **76**, 89–112. (doi:10.1017/S0022112076003145)

Cox, D. R. & Isham, V. 1980 *Point processes*. London, UK: Chapman and Hall.

Driedonks, A. G. M., Van Dop, H. & Kohsiek, W. H. 1978 Meteorological observations on the 213 m mast at Cabauw, in the Netherlands. Prepr. 4th AMS Symp. Meteor. Obs. Instr. (Denver), pp. 41–46.

Farge, M. 1992 Wavelet transforms and their applications to turbulence. *Ann. Rev. Fluid Mech.* **24**, 395–457. (doi:10.1146/annurev.fl.24.010192.002143)

Goel, M. & Srivastava, H. N. 1990 Monsoon trough boundary layer experiment (MONTBLEX). *Bull. Am. Meteorol. Soc.* **71**, 1594–1600. (doi:10.1175/1520-0477(1990)071<1594:MTBLE>2.0.CO;2)

Guala, M., Hommema, S. E. & Adrian, R. J. 2006 Large-scale and very-large-scale motions in turbulent pipe flow. *J. Fluid Mech.* **554**, 521–525. (doi:10.1017/S0022112006008871)

Hoyas, S. & Jimenez, J. 2006 Scaling of the velocity fluctuations in turbulent channels upto $Re_\tau = 2003$. *Phys. Fluids* **18**, 011 702. (doi:10.1063/1.2162185)

Kailas, S. V. & Narasimha, R. 1994 Similarity in VITA-detected events in a nearly neutral atmospheric boundary layer. *Proc. R. Soc. A* **447**, 211–222. (doi:10.1098/rspa.1994.0136)

Kaimal, J. C. 1990 Basic tests for checking validity of field data. WPL Application Note. No. 5.

Kaimal, J. C. & Gaynor, J. E. 1983 Boulder atmospheric observatory. *J. Appl. Meteorol.* **22**, 863–880. (doi:10.1175/1520-0450(1983)022<0863:TBAO>2.0.CO;2)

Kaspersen, J. H. & Krogstad, P. A. 2001 Wavelet-based method for burst detection. *Fluid Dyn. Res.* **28**, 223–236. (doi:10.1016/S0169-5983(00)00031-9)

Kline, S. J., Reynolds, W. C., Schraub, F. A. & Runstadler, P. W. 1967 The structure of turbulent boundary layers. *J. Fluid Mech.* **30**, 741–773. (doi:10.1017/S0022112067001740)

Liandrat, J. & Moret-Bailly, F. 1990 The wavelet transform: some applications to fluid dynamics and turbulence. *Eur. J. Mech. B: Fluids* **9**, 1–19.

Lu, S. S. & Willmarth, W. W. 1973 Measurements of the structure of the Reynolds stress in a turbulent boundary layer. *J. Fluid Mech.* **60**, 481–511. (doi:10.1017/S0022112073000315)

Narahari Rao, K. N., Narasimha, R. & Badri Narayan, M. A. 1971 The "bursting" phenomenon in a turbulent boundary layer. *J. Fluid Mech.* **48**, 339–352. (doi:10.1017/S0022112071001605)

Narasimha, R. 1990 The utility and drawback of traditional approaches. In *Wither turbulence?* (ed. J. L. Lumley), pp. 13–48. New York, NY: Springer.

Narasimha, R. 1995 Turbulence: waves or events? *Curr. Sci.* **68**, 33–38.

Narasimha, R. & Kailas, S. V. 1987 Energy events in the atmospheric boundary layer. In *Perspectives in turbulence studies* (eds H. U. Meier & P. Bradshaw), pp. 88–222. Berlin, Germany: Springer.

Narasimha, R. & Kailas, S. V. 1990 Turbulent bursts in the atmosphere. *Atmos. Environ.* **24**, 1635–1645.

Narasimha, R., Kailas, S.V. & Kaimal J. C. 1990 Turbulent bursts in a near-neutral atmospheric boundary layer. Tech. Memorandum No. 9102, NAL, Bangalore, India.

Narasimha, R., Sikka, D. R. & Prabhu, A. 1997 The monsoon trough boundary layer. Ind. Acad. Sci., Bangalore (referred to as NSP).

Phong-anant, D., Antonia, R. A., Chambers, A. J. & Rajagopalan, S. 1980 Features of the large scale motion in the atmospheric surface layer. *J. Geophys. Res.* **85**, 424–432.

Rajkumar, G., Narasimha, R., Singal, S. P. & Gera, B. S. 1997 Thermal and wind structure of the monsoon trough boundary layer. NSP, pp. 153–170.

Ramage, C. S. 1980 Sudden events. *Futures* **268**, 274.

Rudra Kumar, S., Narasimha, R. & Prabhu, A. 1993 Report 93AS3, Centre for Atmospheric Sciences, Ind. Inst. Sci., Bangalore.

Rudra Kumar, S., Ameenulla, S. & Prabhu, A. 1997 MONTBLEX tower observations: instrumentation, data acquisition and data quality. NSP, pp. 97–124.

Schols, J. L. J. 1984 The detection and measurement of turbulent structures in the atmospheric surface layer. *Bound. Layer Meteorol.* **29**, 39–58. (doi:10.1007/BF00119118)

Schwarz-van Manen, A. D. 1993 Coherent structures over drag reducing surfaces. Ph.D. thesis, Eindhoven Univ. of Tech., Eindhoven, The Netherlands.

Stull, R. B. 1990 *Introduction to boundary layer meteorology.* Dordrecht, The Netherlands: Kluwer Academic Publishers.

Wieringa, J. 1993 Representative roughness parameters for homogeneous terrain. *Bound. Layer Meteorol.* **63**, 323–363.

Willmarth, W. W. & Lu, S. S. 1972 Structure of Reynolds stress near the wall. *J. Fluid Mech.* **55**, 65–92. (doi:10.1017/S002211207200165X)